18th International Conference on Structural Mechanics in Reactor Technology (SMiRT 18)
Beijing, China, August 7-12, 2005
SMiRT18-G02-4

DYNAMIC CRACK GROWTH AND ARREST ANALYSIS USING COHESIVE ZONES

Gilles Debruyne
EDF, LaMSID,
1 av. Du Général de Gaulle 92141 Clamart France
Phone: 00 1-47654575, Fax: 00 1-47654118
E-mail: gilles.debruyne@edf.fr

Miguel Charlotte
LPMTM, Paris XIII University,
av. J-B Clément 93430 Villetaneuse France
Phone: 00 1-49403949, Fax: 00 1-49403938
E-mail: panga973@yahoo.com

ABSTRACT

Crack growth and arrest is a feature of central importance for pressure vessels reliability. One of the main arising questions is the conservative aspect of static analysis versus the dynamic investigation of crack arrest.

In the first part of the paper, the one-dimensional peeling film model is revisited using a Dugdale crack tip condition and compared with a Griffith criterion. This problem is one of the few cases in which all aspects of growth and arrest can be analytically investigated under dynamic assumptions (in particular the crack speed and waves path). In particular, it is shown that in this particular problem, the quasi-static approach is not conservative.

In a second part, the same problem is numerically solved in 2D with finite elements (the film is simulated by a strip of quadrilateral elements and cohesive zones with a Barenblatt law are considered for the peeling moving surface). For a given material toughness, the influence of the Barenblatt critical stress is examined.

At last, prospective simulation of underclad flaw damage growth and arrest in a pressure vessel of PWR, using cohesive elements, is performed. This latter is submitted on a transient thermomechanical loading, which leads to damge initiation, growth and arrest of an undercladding crack (but no fracture growth occurs). An axisymetric model is considered and cohesive zones in the framework of dynamic analysis are used in the plane of initial crack (this latter is assumed running without kinking or deviating out og this plane).

Keywords: Fracture, Dynamic, Crack arrest, Cohesive zones.

1. Introduction

Service life extension of PWR vessels is an important issue for a number of nuclear operators. This aim is partially subjected to improvement of safety margins. These margins may be enhanced by acceptance of a limited amount of crack growth, starting from the initial flaw. It is therefore necessary to predict not only the crack initiation but also the crack arrest. The possible suddenness of the propagation and arrest, due to the variation of toughness of a few part of the vessel by neutron irradiation and collapse of temperatures may involve

important dynamic effects. Analytical investigations for actual structures are very complex to carry on, so that an academic problem analysis may be useful to understand the different features of dynamic crack propagation and arrest. The peeling of a thin film bonded on a rigid surface is a good example to check such features. This problem has been analyzed in a dynamic way by Freund (1989) with a Griffith criterion. It is revisited here with some slightly different conditions, where the film peeling activates a surface energy (a Griffith or a Dugdale-Barenblatt surface energy is considered here). The analytical results are compared with a FE model using cohesive zones.

This cohesive zone model is then applied to the study of a vessel shell ring submitted to a PTS event on the inner cladding surface. This latter is affected by a 6mm depth subclad flaw, which is assumed to be circumferential all around the ring. Therefore, an axisymetric modeling of the vessel is proposed. A previous study for integrity assessment has been performed, by Masson et al (2002).

The base metal is A508 steel, the cladding is an A309L-A308L austenitic steel. Each material mechanical behaviour is described by a linear temperature dependent elastic model.

2. Peeling problem.

2.1. Problem statement.

A thin elastic film of lineic mass ρ initially completely bonded to a rigid plane and stretched by a tension force N is considered. It is submitted on one edge, to an increasing transverse small deflection $u_0(t)$ of constant rate V_0, and suddenly stopping at time T_0. Geometry and loading are such that a one dimension problem may be considered and each material point is designed by $x \in \mathbb{R}^+$, the peeling running on the length $\ell_1(t)$. The main unknown is the deflection $u(x,t)$ (cf. fig. I). The peeling activates a lineic energy $\gamma(u)$, independent on the x position (an homogeneous toughness is considered for the material), but whose the shape fits with the peeling criterion (here Griffith criterion or Dugdale-Barenblatt model where $\ell_2 - \ell_1$ is the cohesive zone length).

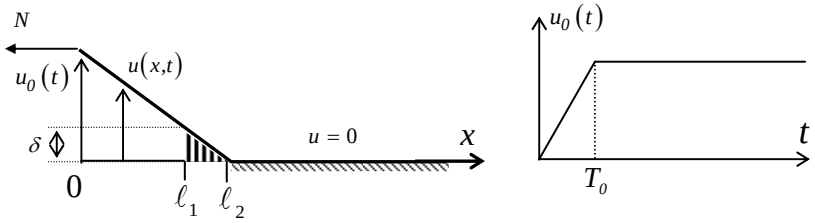

Figure I. Diagrammatic view of the peeling of a thin streched film.

2.1. 1. General formulation

Initial and kinematic conditions are the following :

$$\text{for } x > 0\,,\ \begin{cases} u(x,0) = 0 \\ u_{,t}(x,0) = 0 \end{cases} \quad [1]$$

$$u(0,t) = u_0(t) = \begin{cases} V_0 t, \forall t \in [0, T_0] \\ V_0 T_0, \forall t > T_0 \end{cases} \quad [2]$$

$$u(x,t) \geq 0, \forall x \geq 0, \forall t \geq 0 \quad [3]$$

$$u(x,t) = 0, \forall x \geq \ell_2(t) \quad [4]$$

$u(x,t)$ is continuous on the space-time domain, but the partial derivatives $u_{,x}$ and $u_{,t}$ may be discontinuous on special regular lines C_h, such that a normal vector $\vec{n}_h = (n_{hx}, n_{ht})$ is defined on it by: $C_h : \lambda \in [0,1] \rightarrow (x_h(\lambda), t_h(\lambda))$. On these lines, compatibility of velocities and deformation jumps are (Hadamard conditions) :

$$n_{hx} [\![u_{,t}]\!](x_h, t_h) = n_{ht} [\![u_{,x}]\!](x_h, t_h) \quad [5]$$

The ingredients for the energy balance are : potential energy $P(u) = \frac{1}{2} \int_{\mathbb{R}^+} c^2 \rho u_{,x}^2(x,t) dx$ [6] ($c = \sqrt{\frac{N}{\rho}}$, is the wave speed), kinematic energy $E_C(u) = \frac{1}{2} \int_{\mathbb{R}^+} \rho u_{,t}(x,t) dx$ [7] , and the peeling energy $E_S(u) = \int_{\mathbb{R}^+} \gamma(u) dx$, with $\gamma(u) = \begin{cases} \sigma_c u, if\ 0 \le u \le \delta \\ G_c, if\ u > \delta \end{cases}$ [8] ; this energy density fits with Griffith criterion if $\delta = 0$ and with Dugdale model if $\delta \neq 0$. $\ell_1(t)$ is the broken zone length, with $u(\ell_1(t), t) = \delta, \forall t \ge \frac{\delta}{V_o}$, and $\ell_2(t)$ is the extended damaged zone length (cf; fig.I). For the Griffith case $\ell_1 = \ell_2$.

2. 2. Evolution laws.

Evolution laws of the peeling come from momentum balance : $\rho\left(c^2 u_{,xx} - u_{,tt}\right) = \gamma_{,u}$ [9], for regular points (x,t) of $\Omega \backslash \bigcup_h C_h$ and from Rankine-Hugoniot relation $n_{hx} c^2 [\![u_{,x}]\!] = n_{ht} [\![u_{,t}]\!]$ [10] for the points (x_h, t_h) belonging to C_h for $h \neq \ell_1, \ell_2$. Relations [10] et [5] involve that C_h are straigth characteristic lines such that $n_{hx} c = \pm n_{ht}$. Furthermore, for the Griffith criterion, relations $\left[G_C - \rho(c^2 - \dot{\ell}_2^2) u_{,x}^2 / 2 \right] \dot{\ell}_2 = 0$ [11]

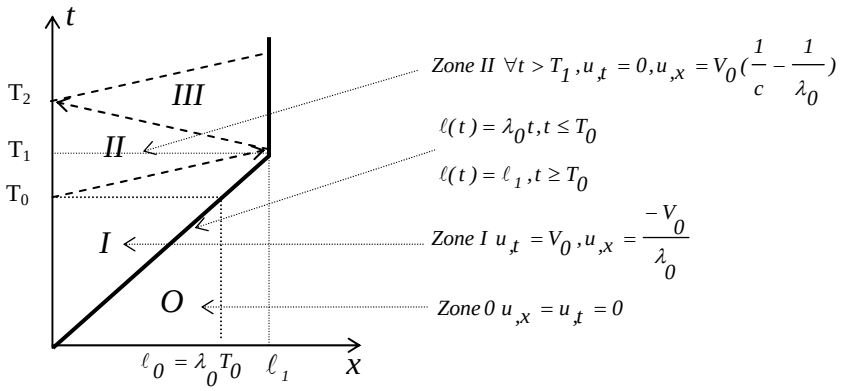

Figure II. Solutions and shock wave path from point (0,T0), for Griffith criterion.

and $G = \frac{\rho c^2}{2}(1 - \frac{\dot{\ell}_2^2}{c^2})u_{,x}^2 \le G_c$ [12], hold on the specific line C_{ℓ_2}, where G is the energy release rate.

2.3. Problem solution with the Griffith criterion.

The expression [11] leads to assert that $\dot{\ell}_2(t) \le c$ since $G_c \ge 0$. The solutions on the interval $[0, T_0]$ are then : $\ell(t) = \lambda_0 t \le \ell_0 = \ell(T_0)$, $u_{,x}(x,t) = -V_0 / \lambda_0$, $u_{,t}(x,t) = V_0$ for $x \le \ell_0$ and $u_{,x}(\ell_0, t) = 0$, $u_{,t}(\ell_0, t) = 0$, with : $\lambda_0 = c / \sqrt{1 + \frac{2G_c}{\rho V_0^2}}$. A jump, due to the sudden loading stopping, appears at the point $(0, T_0)$ propagates on the straight line $x = c(t - T_0)$ and reaches the arrest point $(\ell_a, T_a) = (\frac{c\lambda_0 T_0}{c - \lambda_0}, \frac{cT_0}{c - \lambda_0})$, (cf. fig. II where are listed the solutions in each zone of the characteristics net). The arrest length $\ell_a = V_0 T_0 / (\sqrt{\alpha^2 + \frac{2G_c}{\rho c^2}} - \alpha)$, where $\alpha = V_0 / c$, is more important than the quasi-static predicted length $\ell_a^* = V_0 T_0 / \sqrt{\frac{2G_c}{\rho c^2}}$. Let's notice that when the film is initially partially debonded and subjected to a deflection such that $G = nG_c$, with $n > 1$ as investigated by Freund (1989), the predicted debonded lengths are equal for quasi-static or dynamic analysis. Initial and boundary conditions are therefore crucial as for the conservatism of either of these analyses.

2.4. Some results related to a Dugdale cohesive model.

In this case, the aim is to describe the path of the broken zone $x \le \ell_1$ and of the partially debonded area (cohesive zone) $\ell_1 \le x \le \ell_2$. In this latter, the momentum balance leads to : $\rho(c^2 u_{,xx} - u_{,tt}) = \sigma_c$, where σ_c is a constant strength inside $\ell_1 \le x \le \ell_2$, and null outside. The analysis is limited inside the interval $[0, T_0]$ and we essentially focus on the evolution of $\ell_2(t)$. Up to $T_i = \frac{x_i}{c} = \frac{2V_0 \rho}{\sigma_c}$ (it is supposed that this time is less than the beginning broken time $\frac{\delta}{V_0}$, which involves that the material is not too much brittle or that the deflection rate is not too much higth). The debonding tip $\ell_2(t)$ is a shock wave moving at a speed c . At the point x_i ,two acceleration waves arise. The first one moves backward with the wave velocity c , the second one is the debonding tip $\ell_2(t)$ and moves with a velocity $\dot{\ell}_2 = c/3$, up to the interception with the first one wave which will slow down the tip $\ell_2(t)$. This iterative process (see the figure III) goes on with decreasing

speed $\dot{\ell}_2 = \lambda_{2i} = c/(2i+1)$. The final tip position rounds down the quasi-static one : $\ell^*_2 = c\sqrt{\frac{2V_0\rho t}{\sigma_c}}$. The cohesive zone length at the first broken time is then approximated by : $\Delta\ell = \frac{c}{\sigma_c}\sqrt{2\rho G_c}$

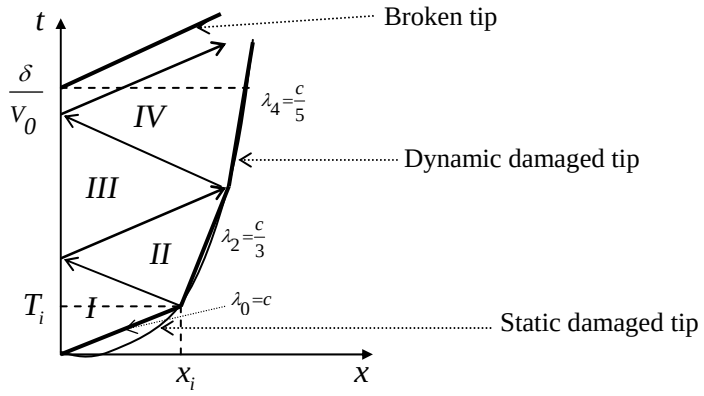

Figure III. Solutions of damaged tip path and acceleration waves from (xi,Ti) for Dugdale criterion.

2.5. Numérical results with Barenblatt cohezive zone model.

The cohesive zone model proposed by Laverne (2004) integrate a Barenblatt law revisited by Francfort and Marigo (1998) in the framework of an energetic theory of Fracture. This law exhibits a surface energy density $\gamma(u) = G_c(1 - e^{-\frac{\sigma_c}{G_c}u})$ slightly different of the Dugdale form(see expression [8]). The figure IV shows the moving tip with speed λ_0 ($\lambda_0 \approx c = 6000m/s$), and the velocity solution in the zone 0 ($u_{,t} = V_0 = 500m/s$), for a ratio $G_c/\sigma_c = 0.02m$ small enough to tend toward the Griffith solution.

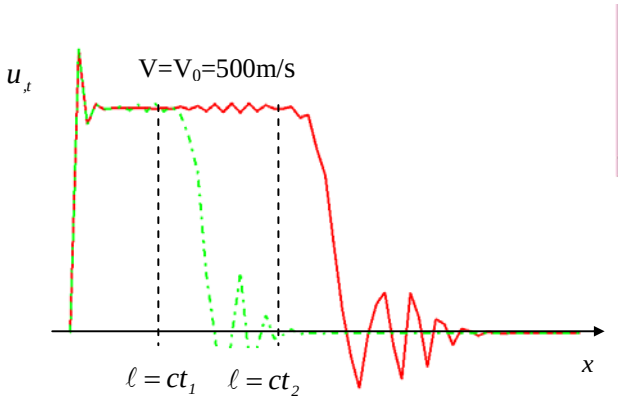

Figure IV. Film velocity for two different times.

3. Underclad flaw growth and arrest analysis using CZM.

3.1. Goal of the analysis.

The aim of this paragraph is the investigation of the behaviour of a subclad flaw in a PWR vessel, during a PTS event, using CZM model under dynamic regime. It's essentially an illustration of the CZM ability to predict fracture and damage growth (the material data do not exactly fit with the actual data), and not really a will to assess RPV structural integrity. This assessment has been already performed, in particular by Masson et al (2002). In fact, it is confirmed here that no fracture occurs during the PTV event. In other terms, the cohesive elements are only partially opened, and the "damaged" zone may propagate and stop. This is that particular point that is studied here as a prospective analysis.

3.2. Model dimensions, material and loading.

The geometry of the structural component is assumed to be axisymetric, including the circumferencial flaw, as shown in Fig. V.

The main dimensions of the structural component are:

- Internal radius: 1992.5 mm,
- Base metal thickness: 200 mm,
- Cladding thickness: 7.5 mm,
- subclad flaw: 6.2 mm (0.2 mm in the cladding),

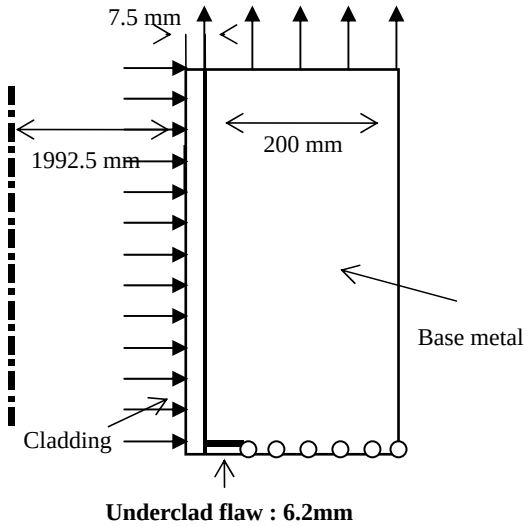

Figure V. Underclad flaw in PWR vessel : schematic representation of half of the model.

The flaw is designed by a blunted crack, the blunted zone being represented by a smooth circle of 0.02mm radius. Both inside the base metal and inside the cladding, cohesive zones, with a Barenblatt law as described in the previous paragraph, lie on all over the. The rest of the component is discretized with isoparametric finite elements.

The base metal is A508 steel while the cladding is an A309L-A308L austenitic stainless steel. Their mechanical properties roughly correspond to conservative values of irradiated material. Young modulus temperature dependence as well as thermal expansion coefficients are reported on Table 1 . The reference temperature is 287°C.

Table 1. thermo-elastic data for base metal and cladding.

Température (°C)	E : Base metal (Gpa)	$\alpha\ °C^{-1}$ Base metal (Tref=287°C)	E: Cladding (Gpa)	$\alpha\ °C^{-1}$ Cladding (Gpa)
0	**205.0**	**1.2867E-5**	**198.5**	**1.7555E-5**
20	**204.0**	**1.3002E-5**	**197.0**	**1.7648E-5**
50	**203.0**	**1.3198E-5**	**195.0**	**1.7788E-5**
100	**200.0**	**1.3521E-5**	**191.5**	**1.8011E-5**
150	**197.0**	**1.3820E-5**	**187.5**	**1.8225E-5**
200	**193.0**	**1.4103E-5**	**184.0**	**1.8575E-5**
250	**189.0**	**1.4382E-5**	**180.0**	**1.8568E-5**
300	**185**	**1.4682E-5**	**176.5**	**1.8768E-5**

The vessel is initially pressurized (16 MPa) and then submitted to a thermal transient applied on the inner cladded surface. The pressure and temperature evolutions with time are reported on Figure VI

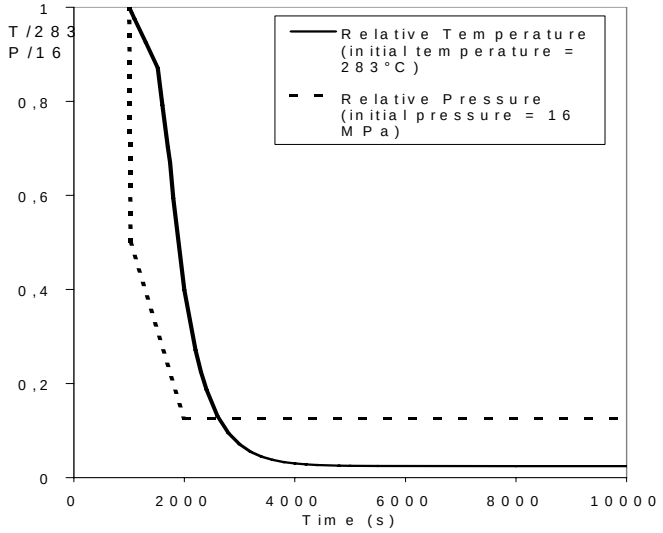

Fig. VI. Evolution of applied temperature and pressure.

The Fracture toughness of base metal is given by the following design curve:

$$\begin{cases} K_{Ic}(MPa\sqrt{m}) = 36.5 + 3{,}1\, e^{0.036(T_B - RT_{NDT} + 55.5)} \\ RT_{NDT}(\Phi = 7.3\,10^{19}\ n.cm^2) = 73°C \end{cases},$$

These values have been carried as cohesive elements surface energy (after transforming them by Irwin formula). For the cladding, an uniform surface energy (no temperature dependence) corresponding to a toughness of $K_{Ic} = 140\ MPa\sqrt{m}$ is considered. The cohesive stress for the base metal cohesive elements varies with temperature from 300 MPa to 500 MPa, and this stress remains constant in the cladding cohesive elements with a value of 300 Mpa.

3.3 Computational aspects and results.

A classical linear transient thermal analysis is performed, then an elastic-dynamic computation is carried on, with an implicit Newmark scheme. All computations are performed by the FE software Code_Aster from EDF. We focus on the mechanical behavior in the vicinity of the flaw. In a first part of the PTS, there is no activation of cohesive element (no fracture and no damage). Then, suddenly, first the cohesive zone inside the cladding activates a little bit but all over the cladding depth. Just after the cohesive zone inside the base metal dissipates energy on a length on a same order than the flaw length (about 6 mm). The damage growth is rather fast (no more than a dozen of seconds to cover the 7.5mm cladding width or the 6mm inside the base metal). The maximum of damage occurs at about 2000 s at the end of the pressure and temperature decreasing (see Fig. VI). The figure VII shows the ratio of surface energy dissipated at this time. The maximum of this ratio is about 0.5 inside the base metal and 0.2 inside the cladding. Consequently, no fracture occurs neither in the cladding nor in the base metal, which matches the previous analysis of this PTS event. But in terms of probability and scenario of Fracture with a more severe

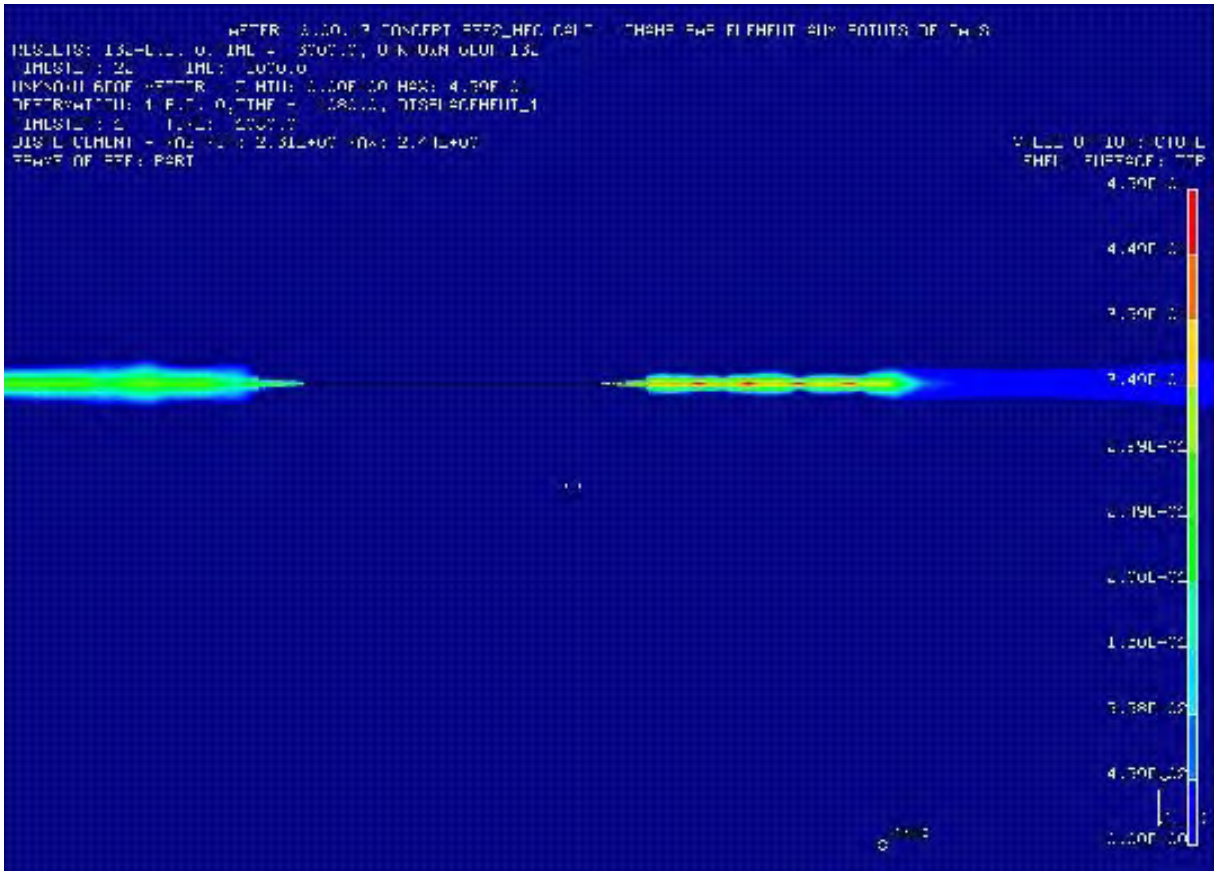

Fig. VII : surface energy ratio dissipated in the cohesive zones of base metal and cladding at time t=2000s.

transient loading, it is interesting to notice that the cladding should yield firstly, then the flaw should grow and stop at an arrest length of the order of the initial length. To prove these assertions, it is necessary to perform a study with CZM for a more severe PTS loading with more realistic data.

4. Conclusions and perspectives

This paper is devoted to dynamic crack growth including cohesive zone model and is roughly divided into two parts :

1) an analytical investigation of an academic problem : the peeling film problem where some exact solutions are exhibited and show the non conservatism of a static approach (in this latter case the crack arrest length is less than the case of dynamic solution). Numerical investigations with CZM fit with the analytical solutions.

2) An application of CZM with a Barenblatt model is applied to the dynamic study of PWR vessel submitted to a PTS loading. This study is simplified by using approximate and not validated material data, and not considering plastic behaviour of the cladding and base metal. Therefore, this study is not a structural integrity assessment. Nevertheless, it is shown that no Fracture occurs during this loading event, which confirms some previous integrity assessment studies, and furthermore this analysis reveals some special points on the damage scenario of the flaw. It is planed, in the near future, to complete this investigation with a more precise material data set, a more realistic transient loading to activate fracture growth, and taken into account an hardening cladding and base metal, with some improvement of the cohesive law (the Barenblatt model with exponential terms involve an artificial damage small tail all along the ligament) and taken in account viscosity in the cohesive behaviour.

REFERENCES

G. A. Francfort, J. J. Marigo (1998) : Revisiting brittle fracture as an energy minimization problem. J. Mech. Phys. Solids, 46 (8), pp. 1319-1342.

L.B. Freund (1989): Dynamic fracture mechanics, Cambridge Monographs on Mechanics and Applied Mathematics

J. Laverne (2004): Formulation Energétique de la Rupture par des modèles de forces cohésives : Considérations Théoriques et Implantations Numériques. PhD thesis Paris 13 University (November 2004).

R. Masson, L. Nicolas, D. Moinereau (2002) : RPV structural integrity assessment during a PTS event : application of an extended Beremin model consistent with WPS test results. ASME PVP Conference, August 2002, Vancouver.

